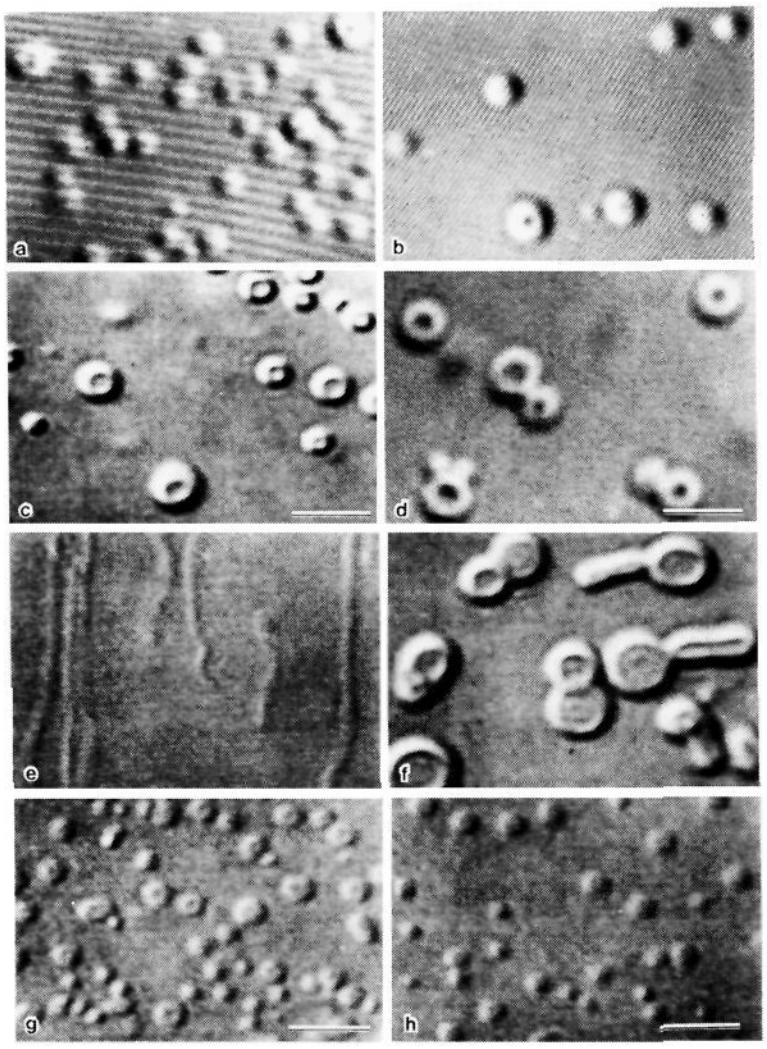

Figure 1. Photographs taken directly from the video screen of spontaneously formed DDA carboxylate vesicles as detected by VEDICM: The vesicles shown by larger than those obtianed from DDAOH although structural transformations remain rapid. (a) DDA acetate 0.13 mM, (b) DDA acetate 0.13 mM, (c) DDA formate 0.13 mM, (d) DDA propionate 0.40 mM, (e) DDA formate 0.13 mM under shear, (f) DDA acetate 0.80 mM at rest after shear, (g) DDA acrylate 5.45 mM sonicated prior to addition of H_2O_2, (h) DDA acrylate 5.45 mM not sonicated prior to addition of H_2O_2. Bar length shown is 2.5 μm and applies to all photographs.

are stable and not merely kinetically favored species. The rapidity of structural transformations in these systems also supports this view.

Other anions examined include trifluoroacetate, trichloroacetate, bromoacetate, benzoate, octanoate, perchlorate, oxalate (as $HC_2O_4^-$), and perfluorobutyrate. These yield birefringent or turbid solutions at 0.1 M and upon dilution; vesicles are not detected. We note in passing the vesicle-forming anions are fairly weak acids (pK_a = 3.9–9.8) while those yielding birefringent or turbid solutions are strong acids (pK_a < 2.7; benzoate (pK_a = 4.2) and octanoate (pK_a = 4.9) are exceptions).

The photographs shown in Figure 1 illustrate a number of features of vesicles formed from the DDA carboxylates. We emphasize these still photographs cannot convey the system dynamics that are directly accessible from the television screen. Figures 1a–d establish that vesicles are formed from DDA carboxylates; whether these relatively small structures are single- or multi-walled cannot be established by VEDICM alone. However, the larger structures shown in Figure 1f certainly appear to be multilamellar vesicles. The carboxylate vesicles are considerably larger than those found with hydroxide as the counterion. Figure 1e illustrates some of the effects of fluid flow and shear on these vesicle systems. The tubules shown in Figure 1e result when the sample is subjected to shear—for example, by moving the coverslip relative to the microscope slide. The tubules slither about and gradually (over ~30 min) revert to the vesicles shown in Figure 1c). Understanding the dynamic response of these vesicles to shear and fluid flow will certainly be important to many potential applications such as controlled drug delivery or tertiary oil recovery.

Regen et al.[10] recently reported stabilized polymer-encased vesicles prepared from dioctadecyldimethylammonium methacrylate. We show similar polymerized vesicles prepared from didodecyldimethylammonium acrylate sonicated (Figure 1g) and unsonicated (Figure 1h) prior to polymerization. The behavior of DDA acrylate monomer is intermediate to that of DDA bromide and DDA carboxylates in that solutions are turbid at high concentration (55 mM) with eventual formation of a surfactant precipitate (in contrast DDA bromide remains finely dispersed), while dilution causes immediate clearing of the solution.

We believe the preliminary results reported here are significant on several counts. Although the relationship between surfactant structure and vesicle stability has received considerable attention, specific counterion effects have remained unexplored. These counterion effects clearly constitute an important means for controlling surfactant microstructure stability and focus attention on the delicate nature of forces that dictate the transitions between bilayers, vesicles, microtubules, and micelles seen in self-assembly systems. The ease of vesicle formation by DDAOH illustrated an important point regarding surfactant self-assembly. However, DDAOH is not easily amenable to careful study; the DDA carboxylates are. The results above, as well as our previous studies on DDAOH, clearly illustrate that subtle chemical or physical differences can lead to pronounced morphological effects when dealing with large-scale aggregates. This has obvious implications regarding our understanding of biological self-assembly as well as on the practical design and utilization of surfactant microstructures.

Acknowledgment. This research was supported by U.S. Army Contract DAA-G29-81-K-0099 (to D.F.E). B.K. acknowledges the support of Dr. T. S. Reese and the National Institutes of Health. J.F.B. thanks Minnesota Mining and Manufacturing Corporation for support as a visiting Postdoctoral Fellow.

Registry No. DDA fluoride, 90790-94-6; DDA formate, 90790-95-7; DDA acetate, 16613-01-7; DDA propionate, 90790-96-8; DDA butyrate, 90790-97-9; DDA glycinate, 90790-98-0; DDA acrylate, 90790-99-1; DDA tartarate (dianion), 90791-00-7; DDA oxalate (dianion), 90791-01-8; DDA trifluoroacetate, 90791-02-9; DDA trichloroacetate, 90791-03-0; DDA bromoacetate, 90791-04-1; DDA benzoate, 90791-05-2; DDA octanoate, 71156-48-4; DDA oxalate (monoanion), 90791-06-3; DDA perfluorobutyrate, 90791-07-4.

(10) Regen, S. L.; Shen, J.-S.; Yamaguchi, K. *J. Am. Chem. Soc.* **1984**, *106*, 2446.

Spin-State Relaxation Dynamics in Iron(III) Complexes: Photochemical Perturbation of the $^2T \rightleftharpoons {}^6A$ Spin Equilibrium by Pulsed-Laser Irradiation in the Ligand-to-Metal Charge-Transfer Absorption Band

Ian Lawthers and John J. McGarvey*

Department of Chemistry
The Queen's University of Belfast
Belfast BT9 5AG
Northern Ireland

Received March 9, 1984

Considerable attention has been devoted recently to investigation of the photophysics and spin-state relaxation dynamics of iron(II) and iron(III) complexes in solution.[1-3] In the case of iron(II) there is substantial evidence[1,2a] that intersystem crossing to lig-

(1) (a) Bergkamp, M. A.; Brunschwig, B. S.; Gütlich, P.; Netzel, T. L.; Sutin, N. *Chem. Phys. Lett.* **1981**, *81*, 147. (b) Creutz, C.; Chou, M.; Netzel, T. L.; Okumura, M.; Sutin, N. *J. Am. Chem. Soc.* **1980**, *102*, 1309. (c) Street, A. J.; Goodall, D. M.; Greenhow, R. C. *Chem. Phys. Lett.* **1978**, *56*, 326. (d) Kirk, A. D.; Hoggard, P. E.; Porter, G. B.; Rockley, M. G.; Windsor, M. W. *Ibid.* **1976**, *37*, 199.

(2) (a) McGarvey, J. J.; Lawthers, I. *J. Chem. Soc., Chem. Commun.* **1982**, 906. (b) Binstead, R. A.; Beattie, J. K.; Dewey, T. G.; Turner, D. H. *J. Am. Chem. Soc.* **1980**, *102*, 6442. (c) Beattie, J. K.; Binstead, R. A.; West, R. J. *Ibid.* **1978**, *100*, 3044. (d) Dose, E. V.; Hoselton, M. A.; Sutin, N.; Tweedle, M. F.; Wilson, L. J. *Ibid.* **1978**, *100* 1141.

(3) Berkgamp, M. A.; Gütlich, P.; Netzel, T. L.; Sutin, N. *J. Phys. Chem.* **1983**, *87*, 3877.

0002-7863/84/1506-4280$01.50/0

Table I. Relaxation Times and Activation Parameters[a] for $^2T \underset{k_{62}}{\overset{k_{26}}{\rightleftharpoons}} {}^6A$ Spin Interconversion in [Fe(XSal$_2$trien)](Y)

X, Y$^-$ (solvent[d])	$\Delta H_{26}^{\ddagger}$	$\Delta H_{62}^{\ddagger}$	$\Delta S_{26}^{\ddagger}$	$\Delta S_{62}^{\ddagger}$	τ_{25},[c] ns	τ, ns[b]	T, K[b]
H, PF_6^- (methanol)[e]	25.6 ± 0.9	10.0 ± 0.9	−12 ± 4	−66 ± 4	5 ± 1	46–192	255–205
H, PF_6^- (acetone)	36.0 ± 0.7	16.7 ± 0.7	28 ± 3	−41 ± 3	3 ± 1	45–250	256–223
5-OCH_3, PF_6^- (methanol–acetone, 10% v/v)	26.0 ± 1.0	8.0 ± 1.0	−7 ± 4	−78 ± 4	5 ± 1	41–233	258–211

[a] $\Delta H^{\ddagger}$, kJ mol^{-1}; $\Delta S^{\ddagger}$, J deg^{-1} mol^{-1}; errors are standard deviations from linear least-squares analyses. [b] Ranges of temperature, T, and measured relaxation times, τ, are shown; average deviation in each τ = ±5% from 3–4 decay traces. [c] τ at 25 °C extrapolated from low-temperature measurements; see text. [d] Less extensive relaxation studies have also been carried out for [Fe(Sal$_2$trien)](PF$_6$) in pyridine and acetonitrile. [e] For [Fe(Sal$_2$trien)](NO$_3$) in this solvent, the ranges of τ and T were 46–194 ns and 261–210 K.

and-field (LF) states figures prominently in the nonradiative decay of the metal-to-ligand charge-transfer excited states. We now report the observation of photochemically initiated perturbation of the $^2T \rightleftharpoons {}^6A$ spin equilibrium in some iron(III) complexes, following pulsed-laser excitation in the ligand-to-metal charge-transfer (LMCT) absorption band. Aside from its intrinsic interest, vis-a-vis the photophysics of the LMCT excited states[3] of iron(III), the phenomenon has the important practical consequence of significantly extended scope for the investigation of $^2T \rightleftharpoons {}^6A$ relaxation dynamics in solution.

The species concerned here are complexes of iron(III) with hexadentate salicylaldehyde–triethylenetetramine ligands [Fe(XSal$_2$trien)](Y), with X = H or OCH_3 and Y$^-$ = PF_6^- or NO_3^-, which have been shown[4] to exhibit low-spin (^2T) $\rightleftharpoons$ high-spin (^6A) isomerism in a range of solvents. Argon-purged solutions of the complexes (Table I) were excited at 530 nm with a Q-switched Nd^{3+}/glass laser[5] (typical pulse energy and duration, 10 mJ, 10–20 ns) and transient absorbance changes in the wavelength range 400–620 nm monitored with a pulsed xenon arc and fast photomultiplier.

The following observations relate to the complex [Fe(5-OCH_3Sal$_2$trien)](PF$_6$) in the solvent mixture methanol–10% acetone (v/v) but are typical of the other systems investigated. Laser excitation at 530 nm resulted in a fast, detector response time limited increase (ΔA) in sample absorbance at 490 nm followed by an exponential decay. The effect was close to detectability limits at temperatures >0 °C, but below this the amplitude increased markedly with further decrease in temperature, ΔA_{max} still being attained within the detector rise time, even at −70 °C. Concomitant ground-state depletion was detected at λ < 420 nm. Figure 1 shows a typical transient at 490 nm and also the transient difference spectrum derived from the initial amplitudes of relaxation traces monitored over the range[6] 400–610 nm. Relaxation times τ were independent of monitoring wavelength in this range and also of sample concentration [(1.5–4.5) × 10^{-4} mol dm^{-3}] but varied with temperature (Table I).

The laser excitation wavelength (530 nm) lies within the LMCT absorption region of the [Fe(XSal$_2$trien)](Y) complexes. Since the amplitude of the fast-rising ΔA signal is greatest at the lowest sample temperatures where the spin equilibrium favors the ^2T isomer, it appears that the effect is due to excitation of this species. Figure 1 shows that the transient difference spectrum matches the temperature difference spectrum (Δt = 17 °C) of the same sample. We therefore attribute the rapid buildup of ΔA to creation of a nonequilibrium population of the ^6A isomer as a result of fast intersystem crossing from the LMCT state expected[3] to be initially populated by laser excitation of the ^2T isomer. The exponential decay is assigned to thermal relaxation of the $^2T \rightleftharpoons {}^6A$ spin equilibrium. In support of this assignment, extrapolation of the low temperature τ data (Table I) to 25 °C leads to values of 3 ± 1 ns and 5 ± 1 ns for the relaxation times in acetone and methanol, respectively, in satisfactory accord with τ (25 °C) = 5.3 ns for the spin-state relaxation of [Fe(Sal$_2$trien)](NO$_3$) in water, from independent ultrasonics studies.[2b]

It has been suggested[3] that the short (~9 ps) lifetimes observed for LMCT excited states of iron(III) polypyridine complexes may

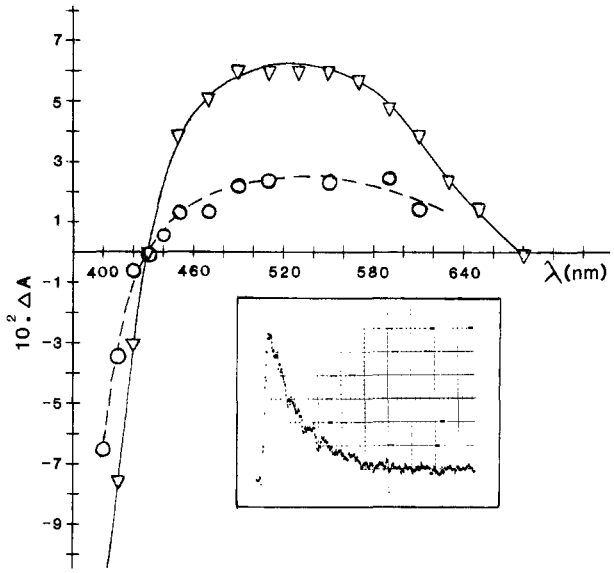

Figure 1. Transient absorbance difference (ΔA) spectrum (○) at −43 °C and temperature difference spectrum (▽) between 20 and 37 °C for [Fe(5-CH_3OSal_2trien)](PF$_6$)$_5$ in methanol–10% acetone. (Inset) Pulsed-laser-induced absorbance change (ΔA) at 490 nm as a function of time in same sample as above at −49 °C. Ordinate, 0.4% ΔA/division; abscissa, 100 ns/division.

be due to the intervention of lower-energy LF states in the deactivation pathway. The present observations of prompt formation of high-spin (^6A) LF states following initial excitation to an LMCT state are consistent with this suggestion. The potential surface of the ^6A state acts as a "trap" for the initially populated LMCT state, although prior involvement of higher energy LF states cannot be excluded on the basis of our (nanosecond time scale) studies. The photophysical picture that emerges resembles that proposed[7] for the picosecond relaxation of an iron(III) porphyrin excited state, in which a "bottleneck" triplet state of the porphyrin ring is suggested to intervene.

On the basis of the above assignment of the relaxation following photochemical perturbation, the measured τ values in the range[8] −15 to −70 °C were combined with thermodynamic data[4] for the

$$^2T \underset{k_{62}}{\overset{k_{26}}{\rightleftharpoons}} {}^6A$$

equilibrium to calculate the spin relaxation rate constants k_{26} and k_{62} as a function of temperature. Table I shows the corresponding activation parameters $\Delta H^{\ddagger}$ and $\Delta S^{\ddagger}$ derived from plots of log (k/T) vs. $1/T$ according to the Eyring equation, with the transmission coefficient κ set equal to unity. The pronounced differences in the activation parameters for the relaxation in methanol and acetone suggest that the solvent plays a significant role in the interconversion dynamics, possibly via spin-state related H-bonding interactions[4] with coordinated N–H groups of the Sal$_2$trien ligand. The importance of solvation effects on the

(4) Tweedle, M. F.; Wilson, L. J. *J. Am. Chem. Soc.* **1976**, *98*, 4824.
(5) (a) Lockwood, G.; McGarvey, J. J.; Devonshire, R. *Chem. Phys. Lett.* **1982**, *86*, 127. (b) Amir-Ebrahimi, V.; McGarvey, J. J. *Inorg. Chim. Acta.*, in press.
(6) Laser scatter interfered with measurements in the 510–540-nm region; an isosbestic point was observed at ca. 430 nm.
(7) Cornelius, P. A.; Steele, A. W.; Chernoff, D. A.; Hochstrasser, R. M. *Chem. Phys. Lett.* **1981**, *82*, 9.
(8) In this range, convolution of the transient decay trace with the detector response function is minimal. Relaxation was observable at t > −15 °C but with lower signal/noise ratios.
(9) (a) Lawthers, I.; McGarvey, J. J.; Heremans, K.; Toftlund, H., manuscript in preparation. (b) Lawthers, I.; McGarvey, J. J.; Toftlund, H., manuscript in preparation.

dynamics of the analogous spin-forbidden processes in iron(II) complexes is suggested by our recent studies[9] of the pressure dependence of the $^1A \rightleftharpoons {}^5T$ relaxation. We now plan to measure the corresponding activation volumes for spin relaxation in the present series of iron(III) complexes.

Acknowledgment. We thank the S.E.R.C. for support and the Department of Education (N. Ireland) for a Research Award (to I.L.).

Phosphinic Acid Dipeptide Analogues: Potent, Slow-Binding Inhibitors of Aspartic Peptidases

Paul A. Bartlett* and William B. Kezer

Department of Chemistry, University of California Berkeley, California 94720

Received February 16, 1984

The invention of potent, specific inhibitors for the various classes of peptidases is a topic of intense biochemical as well as medicinal interest. For the zinc and serine peptidases, a number of effective strategies have been developed based on the ability of phosphorus-containing amino acid analogues to mimic the unstable tetrahedral intermediates involved in peptide hydrolysis.[1-3] We now describe a phosphorus-containing analogue (**1**) of the amino acid

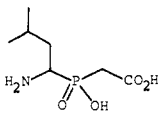

1

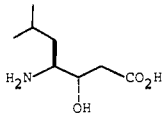

2

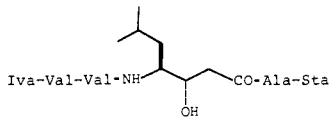

3

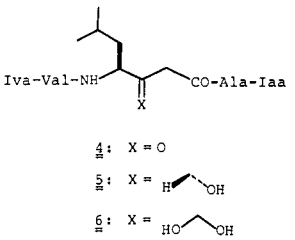

4: X = O

5: X = H, OH

6: X = HO, OH

statine and show that its incorporation into appropriate oligopeptide sequences affords a very tight, slow-binding inhibitor of the prototypical aspartic peptidase pepsin.

The hydroxymethylene group of statine (**2**) may mimic the tetrahedral intermediate that is involved in peptide hydrolysis by the aspartic peptidases, hence oligopeptides such as pepstatin (**3**) that incorporate this amino acid are considered to be transition state analogue inhibitors of these enzymes.[4] Of particular interest is the demonstration by Rich et al. that the keto analogue **4** is bound to the enzyme as a tetrahedral species,[5] possibly the *gem*-diol **6**. Since the equilibrium ketone ⇌ hydrate lies far to the left, the binding energy available to the hydrate is in principle significantly greater than that represented by K_i for the ketone.

Scheme I[a]

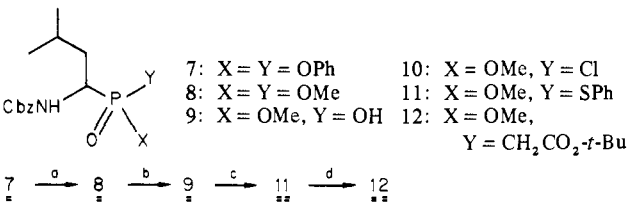

7: X = Y = OPh
8: X = Y = OMe
9: X = OMe, Y = OH
10: X = OMe, Y = Cl
11: X = OMe, Y = SPh
12: X = OMe, Y = CH_2CO_2-*t*-Bu

[a] (a) MeONa, MeOH, 22 °C (84%); (b) NaOH, MeOH, 22 °C (87%); (c) $SOCl_2$, CH_2Cl_2, 22 °C; PhSH, Et_3N, CH_2Cl_2, 22 °C (56%); (d) $LiCH_2CO_2$-*t*-Bu, THF, −78 °C → 0 °C.

Table I. Binding of Tripeptide Analogues to Pepsin

inhibitor	K_i, μM
Iva-D-Sta^P-Ala-Iaa (**15A**)	25[a]
Iva-L-Sta^P-Ala-Iaa (**15B**)	0.9[b]
Iva-L-Sta-Ala-Iaa (**18**)	0.35[c]

[a] Determined at 37 °C at pH 3.5 (0.1 M NaOAc) with Z-His-*p*NO_2Phe-Phe-OMe as substrate. [b] Same as *a* but with Lys-Pro-Ala-Glu-Phe-*p*NO_2Phe-Arg-Leu also as substrate. [c] Reference 11.

It was this surmise that led us to prepare the phosphorus analogue **1**, to mimic the tetrahedral hydrate **6** and take advantage of its additional binding energy.

A suitably protected derivative of "phosphastatine" is prepared as depicted in Scheme I, starting with a phosphonate analogue of leucine, **7**.[6,7] The racemic diastereomers of **11** are readily separated and obtained in pure form by crystallization. Displacement of the phenylthio moiety from each of these diastereomers with *tert*-butyl lithioacetate proceeds stereospecifically and provides the two crystalline diastereomers of phosphinate **12**: **12A**, mp 113–114 °C; **12B**, mp 89–90 °C.

To evaluate the amino acid **1** as a mimic of the hydrate **6**, we incorporated the diastereomer **12A** into two oligopeptide sequences (see Scheme II).[7] Although the starting material **12A** is diastereomerically pure, it is racemic and therefore affords oligopeptides that incorporate both D- and L-enantiomers of phosphastatine.[8] These are differentiated in the course of the synthetic sequences by chromatographic separation of the diastereomers of **14** and **16**, respectively. All four phosphorus-containing peptides **15** and **17** are therefore available in stereochemically pure form.

The phosphorus-containing peptides were evaluated as inhibitors of porcine pepsin by using a spectroscopic assay and either Z-His-*p*NO_2Phe-Phe-OMe (K_m = 0.5 mM, k_{cat} = 0.29 s^{-1}) or the octapeptide substrate Lys-Pro-Ala-Glu-Phe-*p*NO_2Phe-Arg-Leu (K_m = 50 μM, k_{cat} = 100 s^{-1}).[10] Both diastereomers of the triamide **14** proved to be simple competitive inhibitors of porcine pepsin, with binding affinities comparable to those of the analogous statine-containing compound **18** (Table I). The behavior of the diastereomeric tetramides **17** is markedly different: one of the diastereomers (**17A**) is bound more weakly than either of the triamides, whereas the other (**17B**) is one of the most potent inhibitors of pepsin known. We assume that the more potent inhibitor in each pair is that with the L configuration.[8] The modest difference in binding affinity between the two diastereomers of **15**, in contrast to the differences observed between **17A** and **17B**, suggests that the isovaleramido moiety of **15A** can fit into the binding site occupied by the isobutyl side chain of inhibitors with

(1) (a) Bartlett, P. A.; Marlowe, C. K. *Biochemistry* **1983**, *22*, 4618–4624. (b) Jacobsen, N. E.; Bartlett, P. A. *J. Am. Chem. Soc.* **1981**, *103*, 654–657. Jacobsen, N. E.; Bartlett, P. A. *ACS Symp. Ser.* **1981**, *171*, 221.

(2) Lamden, L. A.; Bartlett, P. A. *Biochem. Biophys. Res. Commun.* **1983**, *112*, 1085 and references cited therein.

(3) Weaver, L. H.; Kester, W. R.; Matthews, B. W. *J. Mol. Biol.* **1977**, *114*, 119–132. Kam, C.-M.; Nishino, N.; Powers, J. C. *Biochemistry* **1979**, *18*, 3032–3038. Nishino, N.; Powers, J. C. *Ibid.* **1979**, *18*, 4340–4347. Petrillo, E. W., Jr.; Ondetti, M. A. *Med. Res. Rev.* **1982**, *2*, 1–41. Thorsett, E. D.; Harris, E. E.; Peterson, E. R.; Greenlee, W. J.; Patchett, A. A.; Ulm, E. H.; Vassil, T. C. *Proc. Natl. Acad. Sci. U.S.A.* **1982**, *79*, 2176–2180. Galardy, R. E. *Biochemistry* **1982**, *21*, 5777–5781. Galardy, R. E.; Kontoyiannidou-Ostrem, V.; Kortylewicz, Z. P. *Ibid.* **1983**, *22*, 1990–1995. Monzingo, A. F.; Tronrud, D. E.; Matthews, B. W., personal communication.

(4) Marciniszyn, J., Jr.; Hartsuck, J. A.; Tang, J. *J. Biol. Chem.* **1976**, *251*, 7088–1094. Bott, R.; Subramanian, E.; Davies, D. R. *Biochemistry* **1982**, *21*, 6956–6962.

(5) Rich, D. H.; Bopari, A. S.; Bernatowicz, M. S. *Biochem. Biophys. Res. Commun.* **1982**, *104*, 1127–1133. Rich, D. H.; Bernatowicz, M. S.; Schmidt, P. G. *J. Am. Chem. Soc.* **1982**, *104*, 3535–3536.

(6) Oleksyszen, J.; Subotkowska, L.; Mastalerz, P. *Synthesis* **1979**, 985.

(7) All new compounds were fully characterized by high-field ^1H and ^{31}P NMR; satisfactory combustion analyses were obtained for all neutral compounds.

(8) We have chosen to use the D and L descriptors for the phosphastatine enantiomers to facilitate comparison with the natural amino acids and with statine itself; the L enantiomer of phosphastatine has the *R* configuration at the stereocenter α to phosphorus. The configurations of the phosphastatine moieties in the two series were correlated by separation of the diastereomers of **13** and formation of both **14A** and **16A** from one of them.

(9) Bartlett, P. A.; Johnson, W. S. *Tetrahedron Lett.* **1970**, 4459–4462.

(10) Dunn, B. M.; deLucy, P.; Magazine, H.; Parten, B.; Jimenez, M. In "Peptides: Structure and Function"; Hruby, V. J., Ed.; Pierce Chemical Co.: Rockford, IL, 1984.

0002-7863/84/1506-4282$01.50/0